Methane Activation

International Edition: DOI: 10.1002/anie.201601965
German Edition: DOI: 10.1002/ange.201601965

Spin-Selective Thermal Activation of Methane by Closed-Shell $[TaO_3]^+$

*Shaodong Zhou, Jilai Li, Maria Schlangen, and Helmut Schwarz**

Dedicated to Professor Jose Riveros, Sao Paulo

Abstract: *Thermal reactions of the closed-shell metal-oxide cluster $[TaO_3]^+$ with methane were investigated by using FTICR mass spectrometry complemented by high-level quantum chemical calculations. While the generation of methanol and formaldehyde is somewhat expected, $[TaO_3]^+$ remarkably also has the ability to abstract two hydrogen atoms from methane with the elimination of CH_2. Mechanistically, the generation of CH_2O and CH_3OH occurs on the singlet-ground-state surface, while for the liberation of $^3CH_2$, a two-state reactivity scenario prevails.*

In addition to hydrogen-atom transfer (HAT) promoted by open-shell metal-oxide clusters [Equation (1)],[1] there exist quite a few other reaction patterns with regard to the thermal activation of methane in the gas phase.[2] For example, some bare metal cations are capable of dehydrogenating methane to metal–carbene complexes or isomers thereof, [Equation (2)].[3] Furthermore, a few metal–carbene complexes bring about C–C coupling with methane [Equations (3) and (4)],[3j,k,4] and oxidation of methane can also be achieved with various metal-oxide clusters, thereby generating methanol or formaldehyde [Equations (5) and (6)].[5] Quite unexpectedly, thermal methane activation by closed-shell clusters was recently reported. For example, the cationic oxide $[HTiO]^+$ in its singlet ground state undergoes σ-bond metathesis with methane to release H_2 [Equation (7)].[6] Furthermore, the closed-shell dioxide cluster $[TaO_2]^+$ forms $[Ta(O)(OH)(CH_3)]^+$, and a relativistic effect in forming a strong Ta–CH_3 bond was identified as a driving force.[7] Similarly, the closed-shell clusters $[XHfO]^+$ (X = F, Cl, Br) also give rise to the insertion product $[Hf(X)(OH)(CH_3)]^+$ upon interaction with methane under ambient conditions, and this insertion was traced back to a strong ligand effect of the halogen atom.[8]

Herein, we report a novel type of reaction in which two hydrogen atoms of methane are abstracted by the closed-shell cluster $[TaO_3]^+$, with concomitant release of bare methylene. In addition to this unprecedented process, oxidation of methane to produce methanol and formaldehyde takes place.

$$[M_xO_y]^{\cdot+} + CH_4 \longrightarrow [M_xO_yH]^+ + CH_3^{\cdot} \quad (1)$$

$$[M]^+ + CH_4 \longrightarrow [MCH_2]^+ + H_2 \quad (2)$$

$$[MCH_2]^+ + CH_4 \longrightarrow [MC_2H_4]^+ + H_2 \quad (3)$$

$$[MCH_2]^+ + CH_4 \longrightarrow [M]^+ + C_2H_6 \quad (4)$$

$$[M_xO_y]^+ + CH_4 \longrightarrow [M_xO_{y-1}]^+ + CH_3OH \quad (5)$$

$$[M_xO_y]^+ + CH_4 \longrightarrow [M_xO_{y-1}H_2]^+ + CH_2O \quad (6)$$

$$[HTiO]^+ + CH_4 \longrightarrow [Ti(OCH_3)]^+ + H_2 \quad (7)$$

Under FTICR conditions, the interaction of mass-selected and properly thermalized $[TaO_3]^+$ with CH_4 results in the formation of three product ions [Equations (8)—(10)]. The total reaction efficiency amounts to of 8.6% relative to the collision rate,[9] with a rate constant $k = (5 \pm 1.5) \times 10^{-11}$ cm^3 molecule^{-1} s^{-1}; owing to the uncertainty in the determination of the absolute pressure, an error bar of ±30% has been estimated previously.[10] The background water contributes approximately 20% to the apparent rate constant, which was subtracted to obtain the above mentioned k value. The associated FTICR mass spectra are shown in Figure 1.

$$[TaO_3]^+ + CH_4 \longrightarrow [TaO_3H_2]^+ + CH_2 \quad 60\% \quad (8)$$

$$[TaO_3]^+ + CH_4 \longrightarrow [TaO_2H_2]^+ + CH_2O \quad 38\% \quad (9)$$

$$[TaO_3]^+ + CH_4 \longrightarrow [TaO_2]^+ + CH_4O \quad 2\% \quad (10)$$

The identity of the atoms involved in these reactions was confirmed through labeling experiments. While the $[TaO_3]^+$/CD_4 couple gives only $[TaO_2D_2]^+$ [Equation (9)], from $[TaO_3]^+/CH_2D_2$, the ions $[TaO_2H_2]^+$, $[TaO_2HD]^+$, and $[TaO_2D_2]^+$ are generated in a ratio of 3:8:1. Based on kinetic modeling,[11] this branching ratio can best be reproduced when a kinetic isotope effect (KIE) of 3.0 for the first C–H bond activation step and 1.0 for the second C–H bond activation step is assumed. Interpretation of the data regarding the elimination of methylene [Equation (8)] is more complicated. While $[TaO_3H_2]^+$ is also generated in the reactions of $[TaO_3]^+$ with residual gases present in the ICR cell (Figure 1d), most likely with water (Figure S3 in the Supporting Information), the abundance of $[TaO_3H_2]^+$ is much higher when CH_4 is introduced into the reaction cell (cf. Figures 1a,d). Furthermore, an unexpected signal for $[TaO_3HD]^+$ is generated when $[TaO_3]^+$ is exposed to CD_4 (Figure 1b), thus implying that

[*] Dr. S. Zhou, Dr. J. Li, Dr. M. Schlangen, Prof. Dr. H. Schwarz
Institut für Chemie, Technische Universität Berlin
Straße des 17. Juni 135, 10623 Berlin (Germany)
E-mail: helmut.schwarz@tu-berlin.de
Dr. J. Li
Institute of Theoretical Chemistry, Jilin University
Changchun, 130023 (P.R. China)

Supporting information for this article can be found under: http://dx.doi.org/10.1002/anie.201601965.

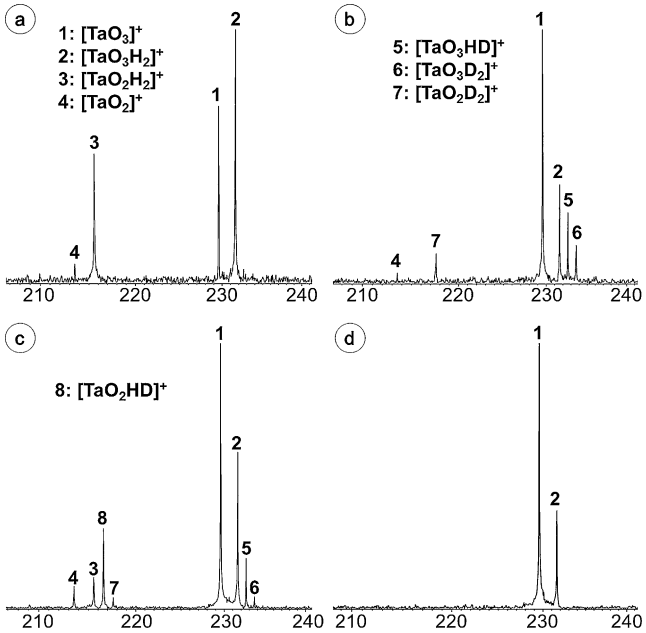

Figure 1. Mass spectra for the reactions of $[TaO_3]^+$ with: a) CH_4, b) CD_4, c) CH_2D_2, and d) argon ($p = 5 \times 10^{-8}$ mbar; reaction delay 5 s). Signal **2** in (d) results from the reaction of $[TaO_3]^+$ with background water, the PESs of which are provided in the Supporting Information. In the discussion of the data, contributions from reactions with background were taken into account.

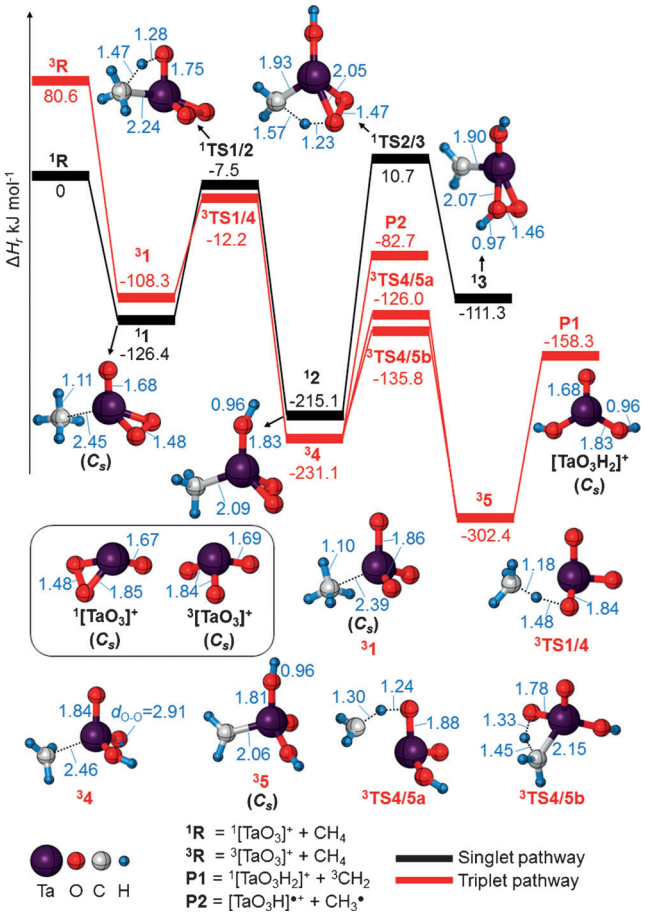

Figure 2. PESs and selected structural information for the generation of $[TaO_3H_2]^+$ from the $[TaO_3]^+/CH_4$ couple as calculated at the CCSD(T)/BSII//PBE0/BSI level of theory. Zero-point corrected energies are given in kJ mol^{-1} and bond lengths in Å; charges are omitted for the sake of clarity.

$[TaO_3HD]^+$ is generated in a secondary reaction. Indeed, H/D exchange processes of $[TaO_3H_2]^+$ with its environment have been demonstrated in independent control experiments. For example, when mass-selected $[TaO_3H_2]^+$ is exposed to CD_4 and CH_2D_2, signals for $[TaO_3HD]^+$ and $[TaO_3D_2]^+$, respectively, are produced (Figures S1 b,c in the Supporting Information). This is in line with theoretical results showing that H/D exchange is exothermic and kinetically feasible under ambient conditions (Figure S2). Nevertheless, the fact that $[TaO_3D_2]^+$ is generated not only by H/D exchange but also in a primary reaction of $[TaO_3]^+$ with CD_4 is clearly demonstrated in a double-resonance experiment. Accordingly, the continuous elimination of $[TaO_3H_2]^+/[TaO_3D]^+$ from the ICR cell does not prevent the formation of $[TaO_3D_2]^+$ from $[TaO_3]^+/CD_4$. Clearly, this product results from the genuine abstraction of two deuterium atoms from CD_4. While it is not possible to derive and determine an intramolecular KIE for the dehydrogenation reaction [Equation (8)] from the relative intensities of the $[TaO_3HD]^+$ and $[TaO_3D_2]^+$ signals, since these product ions are also formed to some extent by subsequent H/D exchange, there is no doubt that $[TaO_3]^+$ is able to dehydrogenate methane with the release of methylene.

The reaction mechanisms were further interrogated with high-level quantum chemical calculations. As shown in Figure 2, the structure of $^1[TaO_3]^+$ differs significantly from that of $^3[TaO_3]^+$, which is 81 kJ mol^{-1} higher in energy. While the former possesses a peroxo ligand with an O–O bond of 1.48 Å, in the triplet state, this bond is cleaved ($d_{O-O} = 2.95$ Å). $^3[TaO_3]^+$ can thus be structurally represented as $[O{=}Ta(O^{\bullet})_2]^+$, with the spin mainly distributed over two oxygen atoms (0.96 for each) and with Ta–O bond lengths of 1.84 Å.

While all transformations in the reaction with methane start from the singlet entrance channel $^1[TaO_3]^+ + CH_4$ (^{1}**R**), the potential-energy surfaces (PESs) of the most favorable pathways for the generation of CH_2 [Equation (8)] involve both the singlet and triplet spin states. Starting from ^{1}**R**, the encounter complex ^{1}**1** is formed through Ta–C interaction, and the H_3C–H insertion intermediate ^{1}**2** is generated via the transition state ^{1}**TS1/2**. The transfer of another hydrogen atom from the so formed methyl group to one of the oxygen atoms of the peroxo group of ^{1}**2** is prohibited by the energetically demanding transition structure ^{1}**TS2/3**. However, along the reaction path, the excited triplet state crosses the singlet surface in a two-state reactivity (TSR) scenario.[12] While we have not located the minimal-energy crossing point,[13] the triplet insertion intermediate is energetically accessible along the sequence ^{3}**1**→^{3}**TS1/4**→^{3}**4**. As mentioned, the high spin density at the oxyl-like oxygen atoms in $^3[TaO_3]^+$ promotes HAT from methane. In ^{3}**4**, the methyl group carries part of the spin (0.62), and the remaining spin is located mostly at an oxyl radical (0.92). Due to the presence of the

latter, yet another HAT from the methyl group to this oxygen atom occurs (^{3}**4**→^{3}**TS4/5a**→^{3}**5**). Interestingly, an alternative transformation via ^{3}**TS4/5b** also exists; in this case, the second hydrogen atom is transferred to the oxygen atom of the Ta=O moiety, and this path is favored by 10 kJ mol^{-1}. In ^{3}**5**, the spin is mainly located at the carbon atom of the methylene group (0.75) and the oxo ligand (1.05). The CH_2 unit coordinates with the metal center through a σ(Ta−C) bond, the homolytic dissociation of which results in the formation of closed-shell $[TaO_3H_2]^+$ and triplet CH_2 (**P1**). Furthermore, liberation of the methyl group from ^{3}**4** to form $[TaO_3H]^{\bullet+}$ is energetically much more demanding compared to ^{3}**TS4/5a** and ^{3}**TS4/5b**. This result is in line with the experimental finding that the product ion $[TaO_3H]^{\bullet+}$ is not observed.

For the other reaction channels [Equations (9) and (10)], the energetically most favorable pathways are confined to the singlet PES (additional information on the transformation on the triplet surface is provided in the Supporting Information). As shown in Figure 3, starting from ^{1}**2**, a methyl rebound step to an oxo ligand takes place to form the stable complex $[Ta(O)(OH)(OCH_3)]^+$ (^{1}**6**), and this intermediate serves as a bifurcation point for the generation of $[TaO_2]^+$ and $[TaO_2H_2]^+$. From ^{1}**6**, either a hydrogen-atom transfer from the methyl group to the oxo ligand takes place via ^{1}**TS6/7** to generate $[Ta(OH)_2(CH_2O)]^+$ (^{1}**7**), or a proton transfer from OH to OCH_3 to form $[TaO_2(CH_3OH)]^+$ (^{1}**8**) occurs via ^{1}**TS6/8**, and dissociations of ^{1}**7** and ^{1}**8** produce the final products

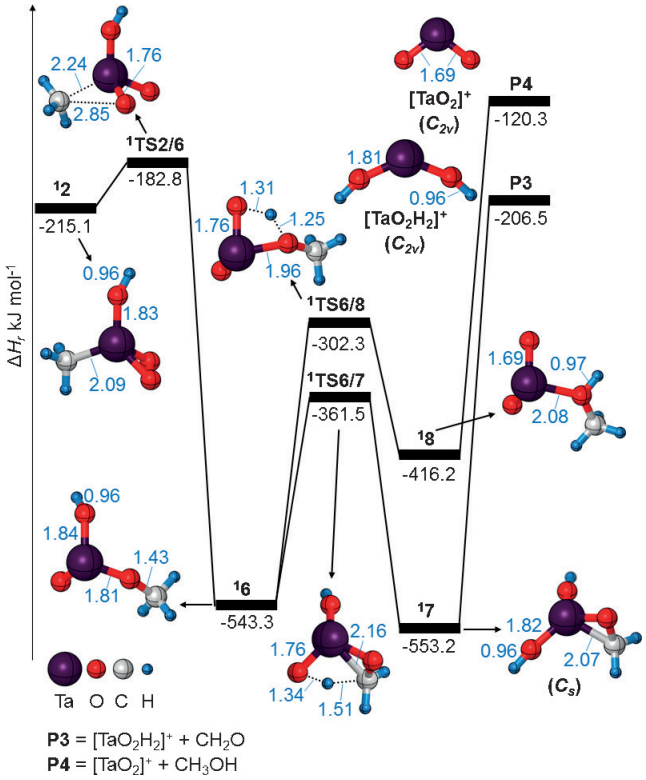

Figure 3. PESs and selected structural information for the generations of $[TaO_2H_2]^+$ and $[TaO_2]^+$ starting from ^{1}**2** as calculated at the CCSD(T)/BSII//PBE0/BSI level of theory. Zero-point corrected energies are given in kJ mol^{-1}, and bond lengths in Å; charges are omitted for the sake of clarity.

$[TaO_2H_2]^+ + CH_2O$ (**P3**) and $[TaO_2]^+ + CH_3OH$ (**P4**), respectively. A conceivable direct methyl transfer from Ta to the hydroxo ligand (^{1}**2**→^{1}**8**) is associated with an energy barrier that is approximately 200 kJ mol^{-1} higher in energy than to ^{1}**TS2/6** and can thus be ruled out. In line with an experimentally calculated KIE of 3.0, ^{1}**TS1/2** corresponds to the rate-limiting step for the formation of formaldehyde (**P3**). The second C−H bond-activation step ^{1}**6**→^{1}**7**, however, does not contribute to the rate-limiting step, which is in line with its KIE of 1.0. In addition, the generation of **P4** is thermochemically much less favored compared to that of **P3**, which is in agreement with the experimental results.

Upon comparing the singlet and triplet states of $[TaO_3]^+$ and the consequences for reactions with CH_4, the most pronounced difference in the structural properties concerns the peroxo ligand O_2^{2-} for the singlet state versus the presence of two oxyl units ($O^{\bullet-}$) in the reactive species of the triplet state. The cleavage of O_2^{2-} into two atomic oxo ligands O^{2-}, promoted by a Au dimer that acts as an electron resevoir, has been described previously in the context of CO oxidation to CO_2.[14] In the present work, cleavage of the O_2^{2-} ligand is facilitated by an intersystem crossing (ISC), and it is this singlet→triplet conversion that opens up the reaction paths to generate $^3CH_2$. While a minimum-energy crossing point has not been located for the formation of $[TaO_3H_2]^+$ in this study, the rather high branching ratio of 60 % indicates that ISC is rather efficient.

According to the computational findings, for the formation of the product couples $[TaO_2H_2]^+/CH_2O$ and $[TaO_2]^+/CH_3OH$, changes in the spin states are not required. Therefore, as has been reported previously for the $[CuO]^+/CH_4$ system, the different product channels owe their existence to spin-selective chemical transformations.[5c]

In summary, the remarkable reactivity of closed-shell $[TaO_3]^+$ towards methane was investigated by using a combination of gas-phase experiments and quantum chemical calculation. In addition to the oxidation of methane to generate methanol and formaldehyde, an unprecedented double hydrogen-atom abstraction was observed. Mechanistic details based on theoretical insight suggest that while the oxidation processes to form CH_2O and CH_3OH take place on the singlet PES, a two-state reactivity scenario[12] prevails in the thermal generation of $[TaO_3H_2]^+$ and $^3CH_2$.

Acknowledgements

Generous financial support by the Fonds der Chemischen Industrie and the Deutsche Forschungsgemeinschaft ("UniCat") is appreciated. We thank Dr. Thomas Weiske for technical assistance.

Keywords: closed-shell cluster · double hydrogen-atom abstraction · gas-phase reactions · methane activation · quantum chemistry

How to cite: *Angew. Chem. Int. Ed.* **2016**, *55*, 7257–7260
Angew. Chem. **2016**, *128*, 7374–7377

[1] Recent reviews on HAT: a) H. Schwarz, *Chem. Phys. Lett.* **2015**, *629*, 91 – 101; b) N. Dietl, M. Schlangen, H. Schwarz, *Angew. Chem. Int. Ed.* **2012**, *51*, 5544 – 5555; *Angew. Chem.* **2012**, *124*, 5638 – 5650; c) W. Lai, C. Li, H. Chen, S. Shaik, *Angew. Chem. Int. Ed.* **2012**, *51*, 5556 – 5578; *Angew. Chem.* **2012**, *124*, 5652 – 5676; d) X.-L. Ding, X.-N. Wu, Y.-X. Zhao, S.-G. He, *Acc. Chem. Res.* **2012**, *45*, 382 – 390; e) Y.-X. Zhao, X.-L. Ding, Y.-P. Ma, Z.-L. Wang, S.-G. He, *Theor. Chem. Acc.* **2010**, *127*, 449 – 465.

[2] Recent reviews on the gas-phase activation of methane: a) H. Schwarz, *Isr. J. Chem.* **2014**, *54*, 1413 – 1431; b) H. Schwarz, *Angew. Chem. Int. Ed.* **2011**, *50*, 10096 – 10115; *Angew. Chem.* **2011**, *123*, 10276 – 10297.

[3] a) V. J. F. Lapoutre, B. Redlich, A. F. G. van der Meer, J. Oomens, J. M. Bakker, A. Sweeney, A. Mookherjee, P. B. Armentrout, *J. Phys. Chem. A* **2013**, *117*, 4115 – 4126; b) P. B. Armentrout, L. Parke, C. Hinton, M. Citir, *ChemPlusChem* **2013**, *78*, 1157 – 1173; c) A. Shayesteh, V. V. Lavrov, G. K. Koyanagi, D. K. Bohme, *J. Phys. Chem. A* **2009**, *113*, 5602 – 5611; d) L. G. Parke, C. S. Hinton, P. B. Armentrout, *J. Phys. Chem. C* **2007**, *111*, 17773 – 17787; e) F. X. Li, X. G. Zhang, P. B. Armentrout, *Int. J. Mass Spectrom.* **2006**, *255*, 279 – 300; f) P. B. Armentrout, S. Shin, R. Liyanage, *J. Phys. Chem. A* **2006**, *110*, 1242 – 1260; g) X. G. Zhang, R. Liyanage, P. B. Armentrout, *J. Am. Chem. Soc.* **2001**, *123*, 5563 – 5575; h) C. Heinemann, R. Wesendrup, H. Schwarz, *Chem. Phys. Lett.* **1995**, *239*, 75 – 83; i) J. K. Perry, G. Ohanessian, W. A. Goddard, *Organometallics* **1994**, *13*, 1870 – 1877; j) K. K. Irikura, J. L. Beauchamp, *J. Phys. Chem.* **1991**, *95*, 8344 – 8351; k) K. K. Irikura, J. L. Beauchamp, *J. Am. Chem. Soc.* **1991**, *113*, 2769 – 2770.

[4] a) S. Zhou, J. Li, X.-N. Wu, M. Schlangen, H. Schwarz, *Angew. Chem. Int. Ed.* **2016**, *55*, 441 – 444; *Angew. Chem.* **2016**, *128*, 452 – 455; b) For a review on the gas-phase chemistry of metal-carbene complexes, see: S. Zhou, J. Li, M. Schlangen, H. Schwarz, *Acc. Chem. Res.* **2016**, *49*, 494 – 502.

[5] a) Y. X. Zhao, Z. Y. Li, Z. Yuan, X. N. Li, S. G. He, *Angew. Chem. Int. Ed.* **2014**, *53*, 9482 – 9486; *Angew. Chem.* **2014**, *126*, 9636 – 9640; b) Z. C. Wang, N. Dietl, R. Kretschmer, J. B. Ma, T. Weiske, M. Schlangen, H. Schwarz, *Angew. Chem. Int. Ed.* **2012**, *51*, 3703 – 3707; *Angew. Chem.* **2012**, *124*, 3763 – 3767; c) N. Dietl, C. van der Linde, M. Schlangen, M. K. Beyer, H. Schwarz, *Angew. Chem. Int. Ed.* **2011**, *50*, 4966 – 4969; *Angew. Chem.* **2011**, *123*, 5068 – 5072; d) A. Božović, S. Feil, G. K. Koyanagi, A. A. Viggiano, X. H. Zhang, M. Schlangen, H. Schwarz, D. K. Bohme, *Chem. Eur. J.* **2010**, *16*, 11605 – 11610; e) M. Pavlov, M. R. A. Blomberg, P. E. M. Siegbahn, R. Wesendrup, C. Heinemann, H. Schwarz, *J. Phys. Chem. A* **1997**, *101*, 1567 – 1579.

[6] R. Kretschmer, M. Schlangen, H. Schwarz, *Angew. Chem. Int. Ed.* **2013**, *52*, 6097 – 6101; *Angew. Chem.* **2013**, *125*, 6213 – 6217.

[7] S. Zhou, J. Li, M. Schlangen, H. Schwarz, *Chem. Eur. J.* **2016**, DOI: 10.1002/chem.201600498.

[8] S. Zhou, J. Li, M. Schlangen, H. Schwarz, *Angew. Chem. Int. Ed.* **2016**, DOI: 10.1002/anie.201602312; *Angew. Chem.* **2016**, DOI: 10.1002/ange.201602312.

[9] M. T. Bowers, J. B. Laudenslager, *J. Chem. Phys.* **1972**, *56*, 4711 – 4712.

[10] D. Schröder, H. Schwarz, D. E. Clemmer, Y. M. Chen, P. B. Armentrout, V. I. Baranov, D. K. Bohme, *Int. J. Mass Spectrom. Ion Processes* **1997**, *161*, 175 – 191.

[11] M. Schlangen, D. Schröder, H. Schwarz, *Helv. Chim. Acta* **2005**, *88*, 1405 – 1420.

[12] a) J. N. Harvey, *WIREs Comput. Mol. Sci.* **2014**, *4*, 1 – 14; b) S. Shaik, *Int. J. Mass Spectrom.* **2013**, *354*, 5 – 14; c) S. Shaik, H. Hirao, D. Kumar, *Acc. Chem. Res.* **2007**, *40*, 532 – 542; d) W. Nam, *Acc. Chem. Res.* **2007**, *40*, 522 – 531; e) P. E. M. Siegbahn, T. Borowski, *Acc. Chem. Res.* **2006**, *39*, 729 – 738; f) S. Shaik, D. Kumar, S. P. de Visser, A. Altun, W. Thiel, *Chem. Rev.* **2005**, *105*, 2279 – 2328; g) H. Schwarz, *Int. J. Mass Spectrom.* **2004**, *237*, 75 – 105; h) S. Shaik, S. P. de Visser, F. Ogliaro, H. Schwarz, D. Schröder, *Curr. Opin. Chem. Biol.* **2002**, *6*, 556 – 567; i) D. Schröder, S. Shaik, H. Schwarz, *Acc. Chem. Res.* **2000**, *33*, 139 – 145; j) S. Shaik, M. Filatov, D. Schröder, H. Schwarz, *Chem. Eur. J.* **1998**, *4*, 193 – 199; k) P. B. Armentrout, *Science* **1991**, *251*, 175 – 179.

[13] J. N. Harvey, M. Aschi, H. Schwarz, W. Koch, *Theor. Chem. Acc.* **1998**, *99*, 95 – 99.

[14] L. N. Wang, Z. Y. Li, Q. Y. Liu, J. H. Meng, S. G. He, T. M. Ma, *Angew. Chem. Int. Ed.* **2015**, *54*, 11720 – 11724; *Angew. Chem.* **2015**, *127*, 11886 – 11890.

Received: February 25, 2016
Revised: March 18, 2016
Published online: May 9, 2016

